

Kang Liu, Xin Jin, Shifen Cheng, Song Gao, Ling Yin & Feng Lu (2023) Act2Loc: a synthetic trajectory generation method by combining machine learning and mechanistic models, *International Journal of Geographical Information Science*, DOI: 10.1080/13658816.2023.2292570

Act2Loc: A Synthetic Trajectory Generation Method by Combining Machine Learning and Mechanistic Models

Kang Liu^{1#*}, Xin Jin^{1, 4#}, Shifen Cheng², Song Gao³, Ling Yin¹, Feng Lu^{2, 4}

¹Shenzhen Institute of Advanced Technology, Chinese Academy of Sciences, Shenzhen China

²State Key Laboratory of Resources and Environmental Information System, Institute of Geographic Sciences and Natural Resources Research, Chinese Academy of Sciences, Beijing China

³Department of Geography, University of Wisconsin-Madison, Madison, WI USA

⁴University of Chinese Academy of Sciences, Beijing China

[#]Kang Liu and Xin Jin contributed equally.

^{*}Corresponding author: kang.liu@siat.ac.cn.

Abstract: Human mobility data play a crucial role in many fields such as infectious diseases, transportation, and public safety. Although the development of Information and Communication Technologies (ICT) has made it easy to collect individual-level positioning records, raw individual trajectory data are still limited in availability and usability due to privacy issues. Developing models to generate synthetic trajectories that are statistically close to the real data is a promising solution. This study proposed a novel trajectory generation method called **Act2Loc (Activity to Location)**, which combined machine learning and mechanistic models. First, an activity-sequence generation model was constructed based on machine learning models (i.e., K-medoids and Transformer) to generate individual activity sequences aligning with human activity patterns. Then, a spatial-location selection model was proposed based on mechanistic models (e.g., Universal Opportunity model) to explicitly determine the specific locations of the activities in each generated sequence. Experimental results showed that compared to baselines based on purely machine learning or mechanistic models, Act2Loc can better reproduce the spatio-temporal characteristics of the real data, with additional advantage of low data requirements for training, proving its potential for generating synthetic trajectories in practice. This research offers new insights on knowledge-guided GeoAI models for human mobility.

Keywords: Trajectory generation, machine learning, mechanistic model, human mobility behavior, activity sequence

1. Introduction

Spatio-temporal trajectories of individuals hold significant implications for various applications such as epidemic simulation, transportation management, and crowd gathering warning (Wang et al., 2021; Dodge et al. 2020; Long et al. 2018). For instance, simulating the movement patterns of suspects and residents can aid in identifying hotspots of criminal incidents, thereby reducing crime rates (Zhu and Wang, 2021); integrating individual movement processes to construct spatially explicit models of disease transmission has become a cutting-edge technique for epidemic prediction and control strategy simulation. (Yin et al., 2021).

The rapid development of modern information and communication technologies (ICTs) in recent years has facilitated the collection of large-scale human mobility data. Various types of actively or passively collected trajectory data, including Global Navigation Satellite Systems (GNSS) records, cellular signaling data, and social media check-ins, have promoted the development of many related fields and yielded significant practical value (Dodge et al. 2020; Yue et al. 2014). However, despite the wide collection of individual trajectory data, its availability is still greatly limited due to concerns regarding personal privacy and data security (Anastasiou et al., 2022; Kamel Boulos et al., 2022). Moreover, the instability of data communication, transmission, and storage devices can often result in data redundancy, loss, and noise, which severely affects the usability of the data. In light of the above problems, generating synthetic trajectories that are statistically close to the real data without recycling real information is a potential solution (Savage, 2023; Pappalardo et al., 2023).

Existing trajectory generation methods can be divided into two categories: *mechanistic models* and *machine learning*. Mechanistic models are mainly studied by researchers in the field of statistical physics. Specifically, researchers firstly uncover the underlying statistical regularities of human mobility by analyzing massive individual spatio-temporal behavior data; then they establish mechanistic models to simulate individual mobility processes to explain the reasons and potential dynamic influences behind these regularities (Barbosa et al., 2018). The main advantage of mechanistic models lies in their ability to explicitly characterize individual mobility processes based on predefined mechanisms, using limited input data and parameters (Brockmann et al., 2006; Gonzalez et al., 2008; Rhee et al., 2011). However, existing mechanistic models are still insufficient in depicting individuals' complex mobility patterns, which results in significant disparities between the generated and the real trajectories. Machine learning (including deep learning) based trajectory generation methods typically construct generative models (e.g., generative adversarial network) based on neural networks (Luca et al., 2021; Rao et al. 2020). Trajectories generated by those data-driven methods tend to closely approximate the real ones because these models can effectively learn the complex and implicit human mobility behavior from the data. However, machine learning methods are usually data-hungry and lack of explainability due to their "black box" nature. Although research on mechanistic models and machine learning has existed for many years, they are still developing independently within their respective domains without effective integration and complementation.

By combining machine learning and mechanistic models, this study proposed a novel trajectory generation method called **Act2Loc (Activity to Location)**. The method firstly employed machine learning models to generate individual activity sequences, then applies mechanistic models to determine the locations of activities in each sequence. The main contributions of this research can be summarized as follows.

(1) An activity-sequence generation model was constructed using two machine learning models, K-medoids and Transformer, to generate individual activity sequences based on clusters of real activity sequence data, which can help capture and preserve the temporal patterns of human daily activities.

(2) A spatial-location selection model was established using mechanistic models, including the advanced Universal Opportunity model for depicting individual's destination selection behavior, to explicitly determine specific locations of activities in each generated sequence, which can enable the reproduction of spatial

characteristics of human mobility behavior.

(3) The proposed method was comprehensively evaluated. The results demonstrated that the proposed method outperforms other trajectory generation methods based on purely machine learning models or mechanistic models as it adaptively combines and leverages the strengths of both.

(4) The proposed method can generate a given number of synthetic trajectories using only small-sample individual activity sequence data and population distribution data, with low data requirements and ease of implementation.

The rest of this paper is organized as follows. Section 2 presents a review on existing studies of trajectory generation methods based on mechanistic models and machine learning. Section 3 provides the mathematical statement of this problem. Section 4 introduces the details of the proposed Act2Loc method. Section 5 describes the experimental results of the case study. Section 6 is devoted to discussions and concludes this work.

2. Literature review

2.1. Trajectory generation methods based on mechanistic models

Based on datasets such as dollar-bill tracking records, mobile phone positioning data, check-in records in social media, and taxi trajectories, researchers in the field of statistical physics have identified statistical regularities of human mobility behavior. For example, researchers found that the jump length of travelers using multiple transportation modes follows power-law or truncated power-law distributions (Brockmann et al., 2006; Gonzalez et al., 2008; Rhee et al., 2011), while the jump length of travelers using single transportation modes follows an exponential or approximate exponential distribution (Liang et al., 2012; Roth et al., 2011). On this basis, researchers modeled the individual mobility process to reveal the underlying microscopic mechanisms behind these macroscopic statistical laws, and thus formed a series of individual trajectory generation models. For instance, Brockmann et al. (2006) proposed the Continuous Time Random Walk (CTRW) model, which incorporates both power-law distributions of jump length and waiting time, to simulate the trajectories of dollar-bills in large-scale geographic spaces. Song et al. (2010) proposed the Exploration and Preferential Return (EPR) model to depict the human behavior mechanism proposed by Gonzalez et al. (2008) that individuals have both inclinations to explore new locations (i.e., unvisited locations) and return to familiar locations (i.e., previously visited locations). Many studies have extended the EPR model by incorporating more complex individual behavioral mechanisms, social mechanisms, and geographic features to better reproduce the statistical patterns (Barbosa et al., 2015; Alessandretti et al., 2018; Dong et al., 2021; Toole et al., 2015; Cornacchia et al., 2021; Pappalardo et al., 2018). However, these models and their variations mainly focus on the spatial characteristics of human mobility and do not adequately consider the spatio-temporal features.

At the intra-urban scale, residents' activities exhibit clear periodic and regular temporal characteristics, such as circadian rhythm and commuting behavior (Eagle et al., 2009; Jiang et al., 2012). To capture both spatial and temporal features of human mobility, researchers have proposed a series of trajectory generation models (Yan et al., 2011; Jiang et al., 2016; Pappalardo et al., 2018; Wang et al., 2019). Two typical models for intra-urban scale are the w-EPR model proposed by Wang et al. (2019) and the DITRAS (DIary-based TRAjectory

Simulator) model proposed by [Pappalardo et al. \(2018\)](#). The w-EPR model incorporates distance decay effects and spatial heterogeneity of population distribution into the exploration phase of the EPR model. However, this model makes a peremptory rule for all individuals to have the same out-of-home duration and determines waiting time for all locations based on a statistical distribution, which is divorced from reality. DITRAS is a trajectory generation framework consisting of a diary generator and a trajectory generator. The diary generator is a data-driven Markov-based model, which generates individual activity diaries by capturing the probabilities of individuals following or breaking their "routine" from the real data. The trajectory generator is an improved EPR model (i.e., d-EPR) that generates locations for each individual diary. However, DITRAS only uses a binary indicator (i.e., staying at home or not) as the "routine" to generate activity diaries, overlooking other prominent activities such as work and others ([Jiang et al., 2012](#)). In addition, the determination of the next activity modeled by the Markov model is only relied on the current activity and independent of historical activities. This "memoryless" property results in the loss of original temporal patterns in the generated activity diaries.

Overall, the advantage of mechanistic models is that they can explicitly characterize individual movement processes based on predefined mechanisms, using limited input data and parameters. However, existing mechanistic models are still insufficient in depicting the complex human mobility behavior, making significant differences between the generated and the real trajectories.

2.2. Trajectory generation methods based on machine learning models

Trajectory generation using machine learning is another mainstream approach primarily concentrated in the field of computer science. Early approaches focused on Markov-based models ([Gambis and Killijian, 2012](#); [Mathew et al., 2012](#); [Chen et al., 2014](#); [Qiao et al., 2015](#)), but such models have limited ability to exploit historical location sequence information, and the predicted position can only be the one that has existed in the historical location sequence. Conventional machine learning methods, such as support vector machines (SVM) and decision trees, require manual definition of features from historical trajectories as model input to predict the next trajectory point ([Baraglia et al., 2013](#); [Muntean et al., 2015](#)).

With the rapid development of deep learning, Recurrent Neural Networks (RNNs), which are widely used for sequence generation tasks such as machine translation and speech recognition, have also been applied in trajectory generation. Long Short-Term Memory (LSTM), a variation of RNNs, has gained widespread popularity due to its ability to address the vanishing gradient problem inherent in traditional RNNs and learn long-term dependencies in sequences ([Berke et al., 2022](#); [Song et al., 2016](#); [Li et al., 2020](#)). When using RNNs as generation models, they are prone to a phenomenon known as exposure bias during the inference stage. This is because the model generates a sequence iteratively and predicts the next token based on its previously predicted ones, which may never have been observed in the training data. This discrepancy between training and inference can accumulate as the sequence progresses, and becomes more pronounced as the length of the sequence increases ([Yu et al., 2017](#)).

To effectively capture useful information from historical trajectory sequence, researchers also introduced

attention mechanism into deep learning models. For example, [Feng et al. \(2018\)](#) used RNNs to capture complex transfer patterns within trajectory sequences, and designed attention modules to capture multi-timescale periodic effects from historical trajectories. Some studies directly exploited attention mechanisms to generate trajectories ([Xia et al., 2021](#); [Feng et al., 2020](#)). For instance, [Xia et al. \(2021\)](#) designed different attention-mechanism neural networks to capture the spatio-temporal dependencies within and between trajectories, and achieved sparse trajectory completion.

In recent years, Generative Adversarial Networks (GANs) have been applied to trajectory generation. Specifically, the generator is responsible for generating trajectories and aims to make the generated trajectories as close as possible to the real ones. While the discriminator performs a classification task, aiming to accurately determine whether the input trajectory is generated or real and provide feedback to the generator to guide its training. Through adversarial learning, both the generator and discriminator improve their performance. [Ouyang et al. \(2018\)](#) constructed a generator and a discriminator both using Convolutional Neural Networks (CNNs), where the generator could directly generate complete trajectories with random noises as input. However, this model had a simple design, limited utilization of effective information, and relatively poor performance. [Rao et al. \(2020\)](#) encoded the spatial, temporal, and semantic information of trajectories and designed a generator and a discriminator that integrated LSTMs. The results showed that given real trajectories and random noises, the generated trajectories effectively achieved the privacy protection goal and well preserved the spatial, temporal, and semantic features of the real trajectories. The aforementioned studies focused on generating trajectories as a whole output. In another GAN structure, the generator operates on a point-by-point sequence generation by using RNN ([Kulkarni et al., 2018](#)), self-attention mechanisms ([Feng et al., 2020](#)), A* algorithm ([Jiang et al., 2023](#)), and others ([Choi et al., 2021](#); [Yuan et al., 2022](#)). As the discriminator needs to perform real/fake classification on the complete trajectories, in these GAN structures, trajectory completion needs to be performed during the intermediate stages. Monte Carlo search is usually used in the discriminator to complete the trajectory based on the currently generated trajectory sequence.

In addition to GANs, Variational Autoencoder (VAE) is also a typical generative model. [Huang et al. \(2019\)](#) proposed a trajectory generation method based on Sequence Variational Autoencoder (SVAE) by combining VAE and Seq2Seq models. The introduction of VAE allows the model to effectively learn human movement patterns from a small amount of trajectory data, thus generating synthetic trajectories that are not exactly the same as the input data but conform to their data distribution characteristics. Recently, [Long et al. \(2023\)](#) proposed a human trajectories generator consisting of user VAE and trajectory VAE, where the former can help learn the user distribution with all human trajectories from a group view, and the latter enables the modeling the complex individual mobility patterns.

The recently emerged Diffusion models have also been applied to trajectory generation tasks ([Zhu et al., 2023](#); [Yuan et al., 2023](#)). For instance, [Zhu et al. \(2023\)](#) applied the Diffusion model to learn spatiotemporal features from real trajectories and generate high-quality trajectories with uncertainty and diversity of human mobility behavior in the real world.

In general, machine learning, especially deep learning, can learn hidden patterns from data using various

ingenious and complex nonlinear methods, making the generated trajectory closer to reality. However, these "black-box" models and purely data-driven approaches also have drawbacks such as poor interpretability, high requirements for training data, complex model structures with numerous parameters, and limited generalization capabilities beyond observed data conditions.

Table 1 summarizes the pros and cons of mechanistic models and machine learning models for trajectory generation. Although the two types of models have complementary advantages, they are still developing independently. To adaptively combine "white-box" mechanistic models with "black-box" machine learning models and leverage the advantages of both would be a beneficial and promising attempt for trajectory generation.

Table 1. Comparison of trajectory generation methods based on mechanistic models and machine learning models.

	Mechanistic models	Machine learning models
Interpretability	Strong	Weak
Fidelity	Low	High
Demand for training data	Low	High
Generalization ability	Strong	Weak
Parameter	Few	Large

3. Preliminary

This section firstly defines individual trajectory and activity sequence, and then formulates the problem of trajectory generation.

Definition. An individual trajectory, denoted as T^k , is defined as a sequence $[l_1^k, \dots, l_N^k]$, where l_i^k denotes the ID of the spatial unit where individual k spent the majority of her/his time during time slot i , i.e., the i th hour from 0:00 of the first observation day. The corresponding individual activity sequence, denoted as A^k , is defined as a sequence $[a_1^k, \dots, a_N^k]$, where a_i^k denotes the type of activity (e.g., "Home", "Work", and "Other") that individual k conducted at spatial unit l_i . N is the total number of time slots considered. For trajectories with a time span of one week, N is equal to 168 (24 hours/day \times 7 days). The spatial units' coordinates are represented by longitude-latitude pairs of their geometric centers.

Problem formulation. Given a real dataset of individual activity sequences $A = [A^1, \dots, A^R]$ and population distribution on spatial units, the objective is to generate a given number of synthetic trajectories $T' = [T^1, \dots, T^G]$ that exhibit similar spatio-temporal characteristics to the real trajectory data.

4. Methodology

In this research, we introduce a novel trajectory generation method called **Act2Loc (Activity to Location)**, as illustrated in Figure 1. Act2Loc consists of two models. The activity-sequence generation model employs machine learning techniques (i.e., a clustering algorithm called K-medoids and a sequence generation model called Transformer) trained with a real activity-sequence dataset. This model can then generate a specified number of synthetic individual activity sequences that follow the temporal patterns of human daily activities in the real data. The spatial-location selection model is built based on mechanistic models that can explicitly

determine the specific locations of human activities in each generated sequence based on population distribution data. Machine learning and mechanistic models are sequentially combined in Act2Loc to capture the temporal and spatial characteristics of human mobility behavior, respectively.

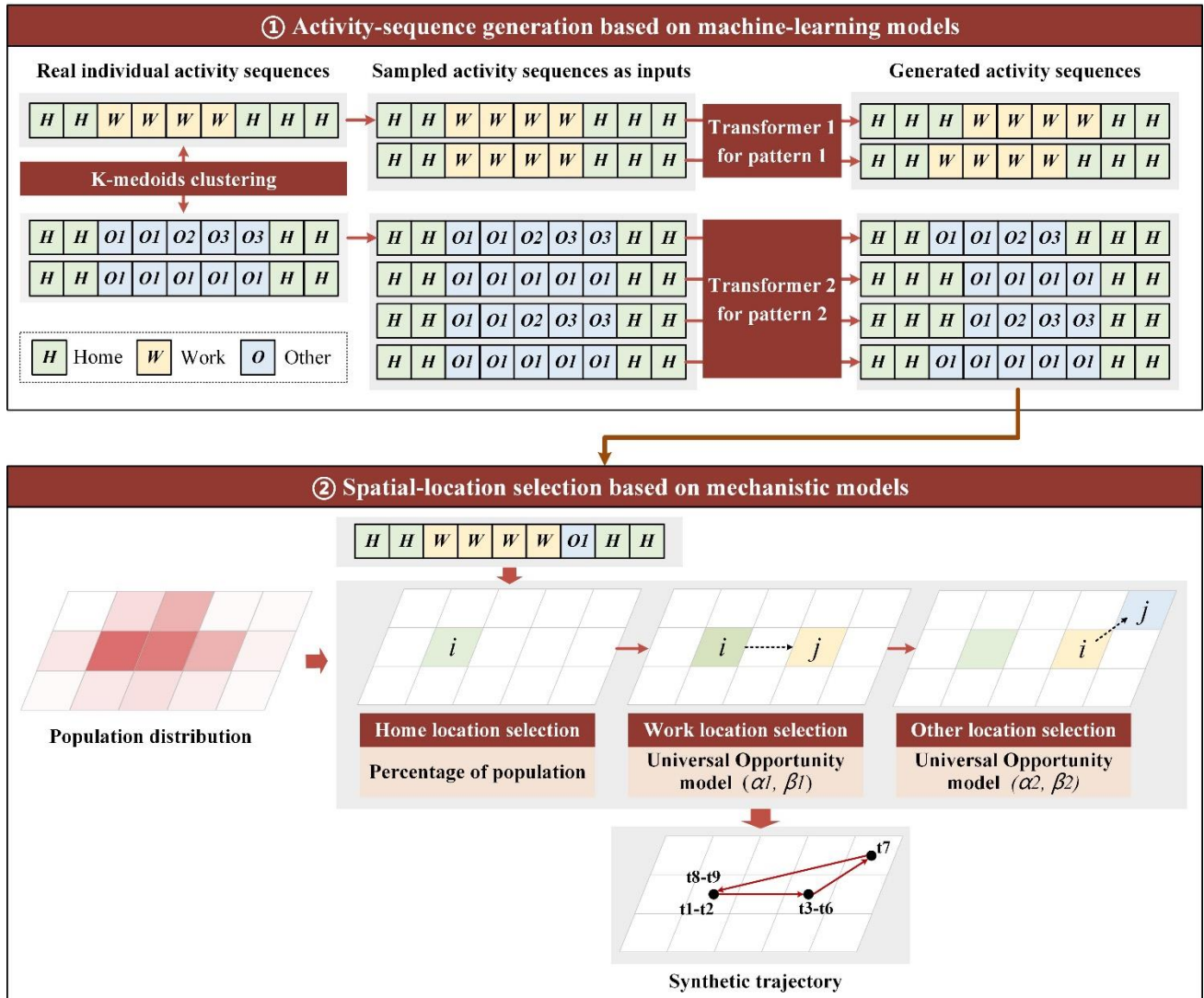


Figure 1. The framework of Act2Loc for synthetic trajectory generation.

4.1. Activity-sequence generation model based on machine learning

Transformer (Vaswani et al., 2017), Recurrent neural networks (RNN) and its variants such as Long Short-Term Memory Networks (LSTMs) and Gated Recurrent Units (GRUs), have been proven effective in sequence modeling and time series forecasting. However, when they are globally trained across all available but heterogenous sequences, the overall accuracy may degenerate. Existing studies have proved that prior subgrouping of time series is able to improve the performance of the baseline RNN models (Bandara et al., 2020).

Considering that human daily activities often exhibit regular routines or temporal patterns (Eagle et al.,

2009; Jiang et al., 2012; Ji et al., 2023), this study adopts a similar idea for generating individual activity sequences. Specifically, we divide the individual activity sequence data into separate clusters using K-medoids algorithm, and then train different activity-sequence generation models based on different clusters of sequence data using Transformer.

4.1.1. Clustering of individual activity-sequence data

We cluster the individual activity-sequence data using the K-medoids algorithm (Kaufman and Rousseeuw, 1990), and select the optimal number of clusters by using the Silhouette coefficient (Rousseeuw, 1987). Through this way, individual activity sequences in the same cluster would have the similar temporal pattern.

K-medoids is a clustering algorithm that is similar to K-means but uses medoids instead of means. A medoid is defined as the data point within a cluster that has the smallest average dissimilarity to all other points in the same cluster. In other words, it is the most centrally located point in the cluster. One advantage of K-medoids over K-means is that it is more robust to outliers since it uses medoids instead of means. Medoids are less sensitive to outliers since they are actual data points in the cluster rather than just the average of all points. Additionally, K-medoids can be used with arbitrary dissimilarity measures, whereas K-means generally requires Euclidean distance. In this study, Levenshtein distance (Levenshtein, 1966), a string metric for measuring the difference between two sequences, is used to measure the distance between two individual activity sequences.

Since residents usually have regular daily routines (Song et al., 2010; Teixeira et al., 2021; Ji et al., 2023), significant clusters can be identified from small samples of individual activity-sequence data (Chen et al., 2016). To generate N trajectories, we need to obtain N activity sequences by randomly sampling with replacement from the real individual activity-sequence data, while preserving the relative proportions of different clusters in the original data.

4.1.2. Construction of individual activity-sequence generation model

For activity sequences in each cluster, we train an attention-based neural network, Transformer (Vaswani et al., 2017), as an individual activity-sequence generation model specifically for that activity pattern. Figure 2 demonstrates the training phase and generation phase of the model. A Transformer consists of an encoder and a decoder. Specially, we add time-ID features to improve the accuracy of the generated activity sequences. The encoder's inputs in both the training and generating phases are the same: the full length of activity sequence $[a_1, \dots, a_{168}]$ and its corresponding time-ID sequence $[t_1, \dots, t_{168}]$ (i.e., chronologically ordered indexes). The decoder's inputs in the training phase activity sequence $[a_1, \dots, a_{167}]$ and its corresponding time-ID sequence $[t_1, \dots, t_{167}]$, while the training target is activity sequence $[a_2, \dots, a_{168}]$.

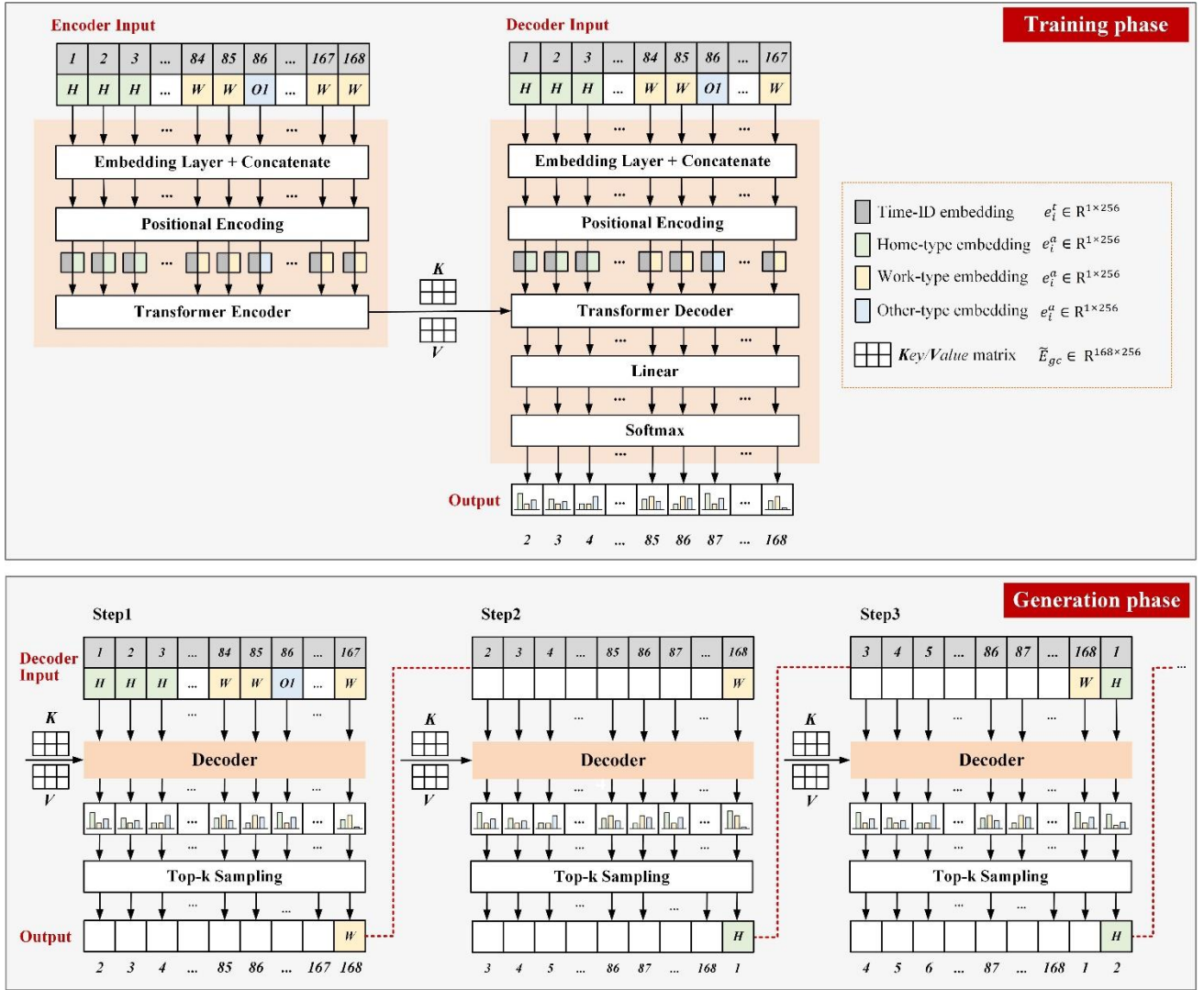


Figure 2. Illustration of individual activity-sequence generation model based on Transformer.

For the embedding layer, we perform embedding on activity-type a_i and time-ID t_i with random matrix $W_a^{N_a \times 256}$ and $W_t^{N_t \times 256}$, where N_a and N_t are the number of unique activity types and time IDs in the activity-sequence dataset. Furthermore, we concatenate the output embeddings:

$$e_i^a = \text{Embedding}(a_i; W_a^{N_a \times 256}), (1)$$

$$e_i^t = \text{Embedding}(t_i; W_t^{N_t \times 256}), (2)$$

$$e_i^{a,t} = \text{concat}(e_i^a, e_i^t) e_i^a, (3)$$

where $\text{concat}(\cdot)$ is a concatenation operator that concatenates two matrices into one; $e_i^a \in \mathbb{R}^{1 \times 256}$, $e_i^t \in \mathbb{R}^{1 \times 256}$ and $e_i^{a,t} \in \mathbb{R}^{1 \times 512}$ are embeddings of activity-type a_i , time-ID t_i and the concatenated results of those two, respectively. Specifically, $e_i^{a,t}$ includes three types of embedding: Home-type embedding, Work-type embedding and Other-type embedding.

To make use of the order of the sequence, we add positional encoding $PE_{(pos,i)} \in R^{1 \times 512}$ to the input embedding $e_i^{a,t}$ in the encoder and the decoder stacks through sine and cosine functions of different frequencies:

$$PE_{(pos,2i)} = \sin\left(\frac{pos}{10000^{\frac{2i}{d_{model}}}}\right), (4)$$

$$PE_{(pos,2i+1)} = \cos\left(\frac{pos}{10000^{\frac{2i}{d_{model}}}}\right), (5)$$

$$\tilde{e}_i = e_i^{a,t} + PE_{(pos,i)}, (6)$$

where pos , i and d_{model} are the position of the activity type in the sequence, the dimension of each feature embedding, and the total dimension of the embedding, respectively. Furthermore, the encoder's input embedding $[\tilde{e}_1, \tilde{e}_2, \dots, \tilde{e}_{168}]$ and the decoder's input embedding $[\tilde{e}_1, \tilde{e}_2, \dots, \tilde{e}_{167}]$ can be represented as $\tilde{E}_{en} \in R^{168 \times 512}$ and $\tilde{E}_{de} \in R^{167 \times 512}$.

Then we use the encoder and decoder to obtain the embedding $\tilde{E}'_{gc} \in R^{167 \times 512}$ for generation. With the Transformer encoder and the embedding $\tilde{E}_{en} \in R^{168 \times 512}$ as input, we gain the embedding $\tilde{E}_{gc} \in R^{168 \times 512}$ enhanced by global activity context and take it as the key ($\mathbf{K} \in R^{168 \times 512}$) and value ($\mathbf{V} \in R^{168 \times 512}$) matrices for the Transformer decoder. The decoder then uses the Multi-Head Self-Attention mechanism to combine the key (\mathbf{K}), value (\mathbf{V}), and the embedding of its input $\tilde{E}_{de} \in R^{167 \times 512}$ to generate the final embedding.

$$\tilde{E}_{gc} = \text{Transformer_encoder}(\tilde{E}_{en}), (7)$$

$$\mathbf{K}, \mathbf{V} = \tilde{E}_{gc}, \tilde{E}_{gc}, (8)$$

$$\tilde{E}'_{gc} = \text{Transformer_decoder}(\tilde{E}_{de}, \mathbf{K}, \mathbf{V}), (9)$$

Finally, the Linear transformation and the Softmax layer are applied to the output of the decoder to obtain the probability matrix $M_{prob} \in R^{167 \times N_a}$ of the target activity sequence. This matrix is then used to train the model with the cross-entropy loss function:

$$M_{prob} = \text{Softmax}(\text{Linear}(\tilde{E}'_{gc})), (10)$$

where each row of M_{prob} corresponds to a probability vector of the activity type in the target activity sequence.

In the training phase, we use Adam as the optimizer and set the learning rate as 0.0001. To avoid the "over-fitting" problem, we adopt the "early stopping" strategy (Prechelt, 1998). The *min_delta* is set as 0.00001 which sets the minimum change in validation loss that counts as an improvement. The patience argument is set as 20 which represents the number of epochs before stopping once the validation loss stops improving.

In the generation phase, the encoder takes the full-length activity sequence $[a_1, \dots, a_{168}]$ and the corresponding time-ID sequence $[t_1, \dots, t_{168}]$ as inputs and produces the key (\mathbf{K}) and value (\mathbf{V}) matrices for the Transformer decoder. For simplicity, we only show the key and value matrices in the figure. The main

difference between the training phase and the generation phase is the decoder inputs. In the first generation step, we feed activity sequence $[a_1, \dots, a_{167}]$ and its corresponding time-ID sequence $[t_1, \dots, t_{167}]$ to the decoder along with the key (\mathbf{K}) and value (\mathbf{V}) matrices and compute the probability matrix M_{prob}^1 . Here, we use $Decoder(\cdot)$ to represent the right part of the model shown in Figure 2, including Embedding Layer, Positional Encoding, Transformer Decoder, Linear Layer and Softmax Layer. Instead of greedy argmax, we use top- k sampling (Ari et al., 2018) as the decoder strategy to increase the diversity of the output, where k is the number of unique activity types. Then we take the last activity type a_{168}^1 of the output sequence $[a_2^1, \dots, a_{167}^1, a_{168}^1]$ and append it to the input of the current generation step $[a_1, \dots, a_{167}]$ to obtain the new input activity sequence $[a_2, \dots, a_{167}, a_{168}^1]$ and its corresponding time-ID sequence $[t_2, \dots, t_{167}, t_{168}]$ for the next generation step. The superscripts of activity types represent the generation step. This process is repeated 169 times until we obtain a brand-new generated activity sequence $[a_1^2, a_2^3, \dots, a_{168}^{169}]$ of a week.

$$M_{prob}^1 = Decoder(a_1, \dots, a_{167}; t_1, \dots, t_{167}; \mathbf{K}, \mathbf{V}), (11)$$

$$[a_2^1, \dots, a_{167}^1, a_{168}^1] = topk_sampling(M_{prob}^1), (12)$$

$$M_{prob}^2 = Decoder(a_2, \dots, a_{167}, a_{168}^1; t_2, \dots, t_{167}, t_{168}; \mathbf{K}, \mathbf{V}), (13)$$

$$[a_3^2, \dots, a_{168}^2, a_1^2] = topk_sampling(M_{prob}^2), (14)$$

...

$$M_{prob}^{169} = Decoder(a_1^2, \dots, a_{166}^{167}, a_{167}^{168}; t_1, \dots, t_{166}, t_{167}; \mathbf{K}, \mathbf{V}), (15)$$

$$[a_1^{169}, a_2^{169}, \dots, a_{168}^{169}] = topk_sampling(M_{prob}^{169}), (16)$$

The hyper-parameters of the Transformer we utilized are listed in Table 2.

Table 2. Hyper-parameters of Transformer model used for individual activity-sequence generation.

Hyper-Parameter	Configuration
Embedding dimension of $d_{activity}$	256
Embedding dimension of d_{time}	256
Embedding dimension of d_{model}	512
Feedforward layer d_{ff}	1024
Encoder layers	8
Decoder layers	8
Dropout	0.2
Label smoothing	0.0
Positional encodings	Fixed absolute sinusoidal
Decoding strategy	Autoregressive top-k sampling
Learning rate	0.0001
Batch size	64
Optimizer	Adam
Loss function	Cross entropy

4.2. Spatial-location selection model based on mechanistic models

We determine the locations (i.e., spatial units) for the activity types in each generated activity sequence based on mechanistic models, which can explicitly describe the individual spatial selection behavior.

4.2.1. Location selection for the “Home” type

Almost all individual activity sequences contain the “Home” type. The probability of a location being selected as an individual’s home location P_i^H is calculated as:

$$P_i^H = \frac{S_i}{\sum S_i}, \quad (17)$$

where S_i is the population of location i , and $\sum S_i$ is the total population of all locations across the study area.

4.2.2. Location selection for the “Work” type

“Home” and “Work” are the most significant and time-lasting activities for most people (Eagle et al., 2009; Jiang et al., 2012), while the locations of other activities such as dining and recreation are typically constrained by home and work locations (Gonzalez et al., 2008; Yan et al., 2011; Wang et al., 2019). Therefore, building upon the determination of home location, we first select work location (if “Work” type exists in the individual activity sequence) and then proceed to choose locations for other activities (if “Other” type exists in the individual activity sequence).

The transition probability for an individual to move from one location to another can be calculated by many mechanistic human mobility models, such as the gravity-based models (Zipf et al., 1946), rank-based models (Noulas et al., 2012), and intervening-opportunity-based models (Stouffer et al., 1940; Simini et al., 2012; Liu et al., 2019; Liu and Yan, 2020). Among those models, we choose the Universal Opportunity (UO) model proposed by Liu and Yan (2020) as our spatial-location selection model for “Work” type. The UO model is an intervening-opportunity-based model that has been proved to have better performance in predicting human mobility at different spatiotemporal scales. As shown in Figure 3, the basic rule of this model is that when individuals choose a destination, they will evaluate the opportunity benefits that all locations will bring to them, and they comprehensively compare the opportunity benefit of the origin, the opportunity benefit of the potential destination, and the benefits of the intervening opportunities. Specifically, the probability of an individual at origin i choosing destination j as the destination is defined as:

$$P_{ij} = \frac{(P_i + \alpha s_{ij})P_j}{[P_i + (\alpha + \beta)s_{ij}][P_i + P_j + (\alpha + \beta)s_{ij}]} \cdot (18)$$

Here, P_i and P_j represent the opportunity benefit of location i and location j , respectively. s_{ij} represents the intervening opportunities between them (excluding P_i and P_j), which refers to the total opportunities within a circle centered at location i with radius equaling to the distance between locations i and j . α is a parameter representing the preference of individuals towards high benefits when choosing locations, and β is another parameter representing the preference of individuals towards short distances when choosing locations. The values of α and β range from 0 to 1, and higher values indicate a higher preference.

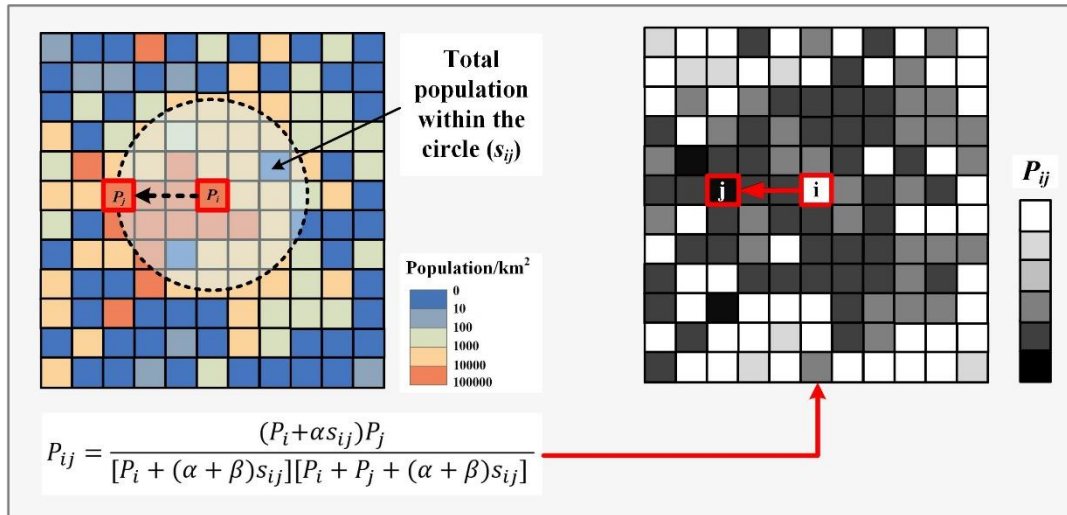


Figure 3. Illustration of the Universal Opportunity (UO) model for location selection.

In terms of selecting the location of “Work” type in each generated individual activity sequence, P_i represents the population of the home location, P_j represents the population of the potential destination j , and s_{ij} refers to the total population (excluding P_i and P_j) within a circle centered at the home location with radius equaling to the distance between the home location and the destination j .

4.2.3. Location selection for “Other” type

Some individual activity sequences contain one or more “Other” types. Similarly, when choosing locations for “Other” type, individuals compare the benefits of her/his current location, the benefits of different potential “Other” locations, and the intervening opportunities. Using the same mechanistic model applied in Section 4.2.2 for work location selection, this study applies equation (18) to calculate the probability of the individual at current location i choosing location j as the destination for “Other” type.

By fitting the real commuting and non-commuting flow data in the study area, this research determines the best preference parameters ($\alpha_1 = 0.13, \beta_1 = 0.61$) for work location selection and the best preference parameters ($\alpha_2 = 0.01, \beta_2 = 0.45$) for other activity location selection. It can be seen that the parameter β is larger than α , indicating that residents have a greater preference for short distance than for high potential benefits in both situations. This phenomenon is particularly significant in the selection of other activity locations compared to the selection of work locations as $\beta_2/\alpha_2 > \beta_1/\alpha_1$, which is consistent with the notion that individuals usually have less flexibility in choosing a nearer workplace and have limited time budget for conducting “Other” activities at a distant place.

5. Results

5.1 Data and processing

We chose Shenzhen City, China as the study area to validate the effectiveness of our proposed method. Located in southern China, Shenzhen is one of the largest and most developed cities in the country. According

to The Seventh National Population Census of Shenzhen City¹, it has a permanent resident population of approximately 17.56 million as of midnight on November 1st, 2020. We divided the study area into 1km grids and used two datasets – population data and trajectory data – for our experiments. The population data was obtained from WorldPop² and comprised the 100m grid population distribution (2020 version). Figure 4 depicts the population distribution of Shenzhen City aggregated at the 1km grids.

The trajectory data was sourced from the Smart Steps³, a big data company under China Unicom, one of the three major telecommunications operators in China, which has large population coverage. Our study utilized trajectories of 200,000 individuals of a week from November 1 to November 7, 2021. Each original trajectory is composed of a sequence of locations in the format of [*uid*, *stime*, *etime*, *lat*, *lng*], where *lat* and *lng* denote the latitude and longitude of the location, while *stime* and *etime* denote the start and end time of the individual stayed at the location. We performed a spatial mapping of trajectory locations to spatial units of the study area, and a temporal mapping of trajectory locations to 1-hour-interval time slots (e.g., 13:00-14:00) of the time span (i.e., a week). If there are more than one location within the same time slot, the location with the longest dwell time was determined as the location for the time slot. After those data preprocessing, each individual trajectory can be represented as a sequence of Grid IDs with a length of 168 (24 hours/day×7 days), as shown in Table 3.

Furthermore, we identified activity types from each trajectory and constructed the corresponding individual activity sequence, a sequence of activity types with the same time interval (i.e., 1 hour) and length (i.e., 168) as the trajectory. Activity types can be identified by the following rules.

- 1) The location where an individual spent the longest time between 21:00 and 6:00 during the week was regarded as her/his home location and labeled as activity type of “Home (H)”.
- 2) We determined an individual’s work location as the place where she/he spent the most time between 9:00 and 18:00 during the week, with the exception of her/his home location. Additionally, we only considered a location to be a work location if the time spent there exceeded 40% of the time spent at the home location. If such a location exists, it was labeled as activity type of “Work (W)”. It should be noted that, if an individual works at the same spatial unit as her home, her work location will be recognized as “Home” type. But this does not affect the generated spatio-temporal trajectories after the spatial-location selection phase. For example, considering an individual whose daily activity sequence is “home (0:00-8:00) – work (8:00-18:00) – home (18:00-24:00)”. If her workplace is located close to her home (in the same 1km grid), our method would identify her activity sequence as “home (0:00-8:00) – home (8:00-18:00) – home (18:00-24:00)” and determine her location between 8:00 and 18:00 as the grid the same with her home, which is still in line with the reality.

¹ http://tj.sz.gov.cn/zwgk/zfxgkml/tjsj/tjgb/content/post_8771927.html

² <https://www.worldpop.org>

³ <http://www.smartsteps.com>

- 3) If a location was neither labeled as “Home (H)”, nor labeled as “Work (W)”, it would be labeled as “Other (O)”. Different other activity locations of the same individual were labeled as “Other1 (O1)”, “Other2 (O2)”, etc., which can reflect the relative richness of different individuals’ daily activities.

Using the above steps, this study constructed 50,000 individual activity sequences from 50,000 individual trajectories randomly sampled from the trajectory dataset with a total of 200,000 individual trajectories.

It is worth noting that in addition to extracting individual activity sequences from trajectory data, it is also possible to extract such sequences from resident travel survey data (Jiang et al., 2012). The latter may include a more diverse range of activity types (e.g., shopping and recreation) and avoid the issue of mistakenly identifying the “Work” type as the “Home” type when workplace and home are close in space.

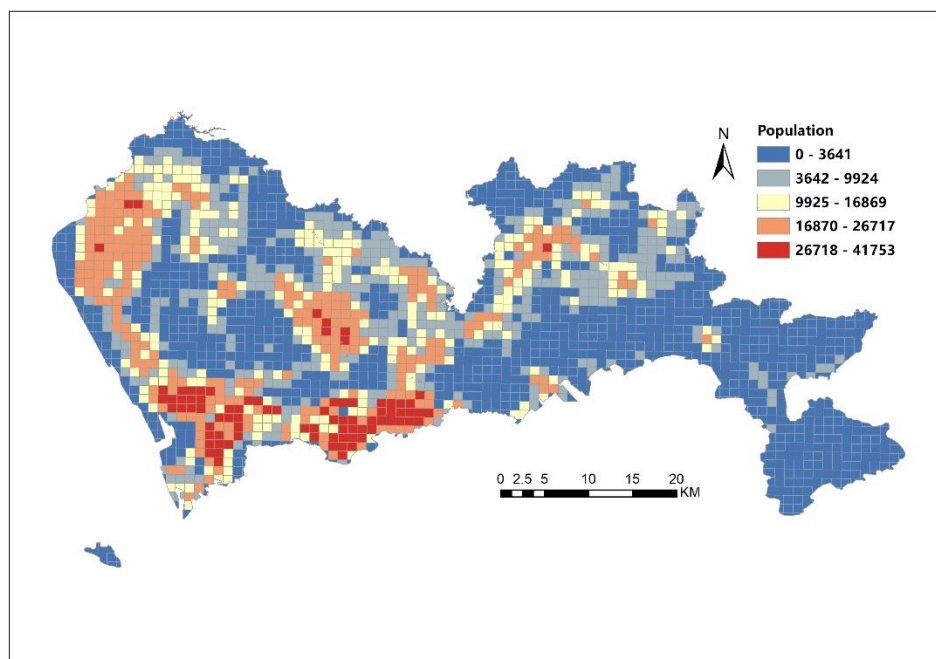


Figure 4. Map of study area and population distribution in 1km grids.

Table 3. Example of an individual trajectory and the corresponding activity sequence of a week.

Time slot	0:00-1:00	1:00-2:00	...	23:00-24:00	00:00-01:00	...	23:00-24:00
Time ID	1	2	...	24	25	...	168
Grid ID	1957	342	...	342	342	...	913
Activity type	Home (H)	Other 1 (O1)	...	Home (H)	Home (H)	...	Other 2 (O2)

5.2. Generation results of individual activity sequences

5.2.1. Evaluation metrics

This study applied BLEU (Bilingual Evaluation Understudy) to evaluate the performance of activity generation model. BLEU is a precision-based metric initially proposed for evaluating the quality of text which has been machine-translated from one natural language to another. It computes the n-gram overlap between the

reference and the candidate sequences:

$$BLEU_n = \frac{\sum_{p \in candidate} \sum_{n-gram \in p} Count_{clip}(n-gram)}{\sum_{p' \in candidate} \sum_{n-gram' \in p'} Count(n-gram')}, (19)$$

where $Count_{clip}(n-gram)$ is clipped by the maximum number of times the given $n-gram$ appears in the corresponding reference sentence. For example, if a particular $n-gram$ appears twice in the candidate, but once at most in the reference, then we consider the matched $n-gram$ count as 1 not as 2. Here we use $BLEU_1$ to compare each generated activity sequence (i.e., the candidate sequence) with the real one (i.e., the reference sequence), and use the averaged value of all real—generated sequence pairs as the evaluation metric for the activity-sequence generation model.

5.2.2. Result analysis

We compared activity sequence generation models with and without prior-clustering by K-medoids. In addition to Transformer utilized in our method, we also selected RNN, LSTM, and GRU as a comparison. Each model generated 50,000 synthetic activity sequences trained on 50,000 real activity sequences by a sequence-to-sequence scheme similar to the Transformer introduced in Section 4.1.2.

Table 4 shows the evaluation results based on the BLEU metric. We can see that all sequence generation models with prior-clustering outperformed those without prior-clustering. This is because the clustering—generation strategy can avoid the dampening effect appeared when heterogenous activity sequences training in the same model. Moreover, Transformer showed an excellent performance even without prior-clustering, proving the suitability of Transformer in modeling human activity sequences.

Table 4. Evaluation of different activity-sequence generation models based on BLEU metric.

Model type	Model	without prior-clustering	with prior-clustering
RNN-based	RNN	0.7037	0.8426
	GRU	0.7056	0.8367
	LSTM	0.6907	0.8513
Attention-based	Transformer	0.9891	0.9954

Figure 5 illustrates the real activity sequences of 50,000 individuals of a week and the corresponding activity sequences generated by Transformer (with prior-clustering) and another comparative model, MarkovDiaryGenerator (MDG), the diary generator of the trajectory generation model DITRAS (Pappalardo et al., 2018). MDG calculates the probabilities of individuals following or deviating from their regular activity patterns and utilizes a Markov-based model to generate individual activity sequences. Since it is not a sequence-to-sequence generation process, we cannot apply the BLEU metric and compare it in Table 4.

As shown in Figure 5(a), for the real activity sequences, the optimal number of clusters is eight and four significant patterns can be identified, which can be described as follows.

- a) “Home-stay” pattern, indicates that individuals’ daily activities are dominated by “Home” type. This pattern accounts for approximately 59.41% of individuals. The “Home-stay” pattern accounts for a

large proportion. This is because activity sequences in our study were identified from the trajectories. If an individual's workplace is in the same spatial unit as her/his home, it will be recognized as "Home" type. However, this would not make a difference on the trajectory generation result based on our proposed spatial-location selection model in Section 4.2.

- b) "996-working" pattern, indicates that individuals' activities from Monday to Saturday (starting at 9:00 AM and ending at 9:00 PM) are dominated by "Work" type. This pattern accounts for approximately 9.64%.
- c) "995-working" pattern, indicates that individuals' activities from Monday to Friday (starting at 9:00 AM and ending at 9:00 PM) are dominated by "Work" type. This pattern accounts for approximately 10.64%.
- d) "965-working" pattern, indicates that individuals' activities from Monday to Friday (starting at 9:00 AM and ending at 6:00 PM) are dominated by "Work" type. This pattern accounts for approximately 7.20%.

Figure 5(b) illustrates that the individual activity sequences generated by Transformer (with prior-clustering) exhibits four significant patterns that are highly similar to the real ones, which obviously has better performance than the Markov-based MDG shown in Figure 5(c). This is because in the Markov-based model, the transition probabilities between two consecutive activity types are based solely on the previous one. As a result, the newly generated activity sequences would overlook the long-term temporal patterns. In contrast, the Transformer has powerful ability in capturing the sequence patterns due to its attention mechanism.

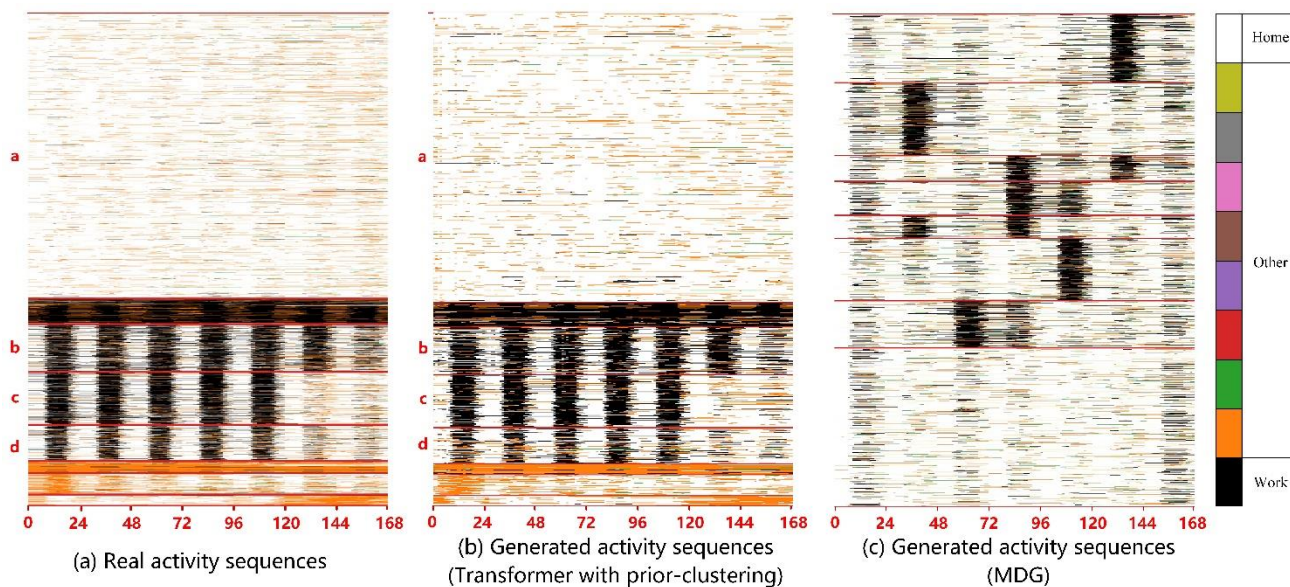


Figure 5. Clustering results of the real and the generated individual activity sequences.

5.3. Generation results of individual trajectories

In this section, we compared our proposed Act2Loc method with the baselines, which are two mechanistic models including DITRAS (Pappalardo et al., 2018) and w-EPR (Wang et al., 2019), and three machine learning models including LSTM, SeqGAN (Yu et al., 2017), and MoveSim (Feng et al., 2020).

As for the Act2Loc, we firstly sampled and generated 200,000 individual activity sequences based on 50,000 real activity sequences using the activity-sequence generation model, and then generated the corresponding 200,000 trajectories using the spatial-location selection model.

5.3.1. Evaluation metrics

Five commonly used metrics are applied to depict the spatiotemporal characteristics of a trajectory dataset (Luca et al., 2021), and the Jensen-Shannon (JS) divergence is used to evaluate the difference in probability distributions of each metric between the real and the generated trajectory data.

- 1) *Duration*: the time consistently spent at the same location visited by an individual.
- 2) *Displacement*: the distance between two consecutive distinct locations visited by an individual.
- 3) *LocNum*: the number of unique locations visited by an individual.
- 4) *Radius*: radius of gyration, the feature distance around the centroid of an individual's trajectory calculated as:

$$r_g = \sqrt{\frac{1}{n} \sum_{i=1}^n (r_i - r_0)^2}, \quad (20)$$

$$r_0 = \sum_{i=1}^n \frac{r_i}{n}, \quad (21)$$

where r_i is the coordinate of trajectory point i , r_0 is the centroid of the trajectory, and n is the number of trajectory points.

- 5) *I-rank*: the visiting frequencies of top-10 locations (sorting in descending order) visited by an individual.

The formula for calculating JS divergence is:

$$JS(p|q) = \frac{1}{2}KL(p|m) + \frac{1}{2}KL(p|m), \quad (22)$$

$$KL(p|q) = \sum_{i=1}^n p_i \log\left(\frac{p_i}{q_i}\right), \quad (23)$$

where p , q and m correspond to the probability distributions of a metric for the real generated trajectory dataset, the generated trajectory dataset, and the average of their sum, respectively. A lower value of JS divergence signifies a greater similarity between the two probability distributions and indicates a higher level of fidelity of the generated synthetic trajectories.

The Common Part of Commuters (CPC) metric is also adopted to measure the similarity of mobility flows between locations that are aggregated from the synthetic and the real trajectories. CPC is calculated as:

$$CPC = \frac{2 \sum_{i=0}^N \sum_{j=0}^N \min(T'_{ij}, T_{ij})}{\sum_{i=0}^N \sum_{j=0}^N (T'_{ij} + T_{ij})}, \quad (24)$$

where T_{ij} is the mobility flow from location i to j aggregated from the real trajectory data, and T'_{ij} is the mobility flow from location i to j aggregated from the generated trajectory data. The CPC metric is bounded between 0 and 1, and a higher value reflects greater consistency between the real and the generated mobility flow, and hence, a higher degree of fidelity of the generated trajectory data.

5.3.2. Overall performance

Table 5 presents the JS divergences toward the five spatiotemporal metrics and the CPC metric. Our proposed Act2Loc method outperforms the baselines in all metrics (with the lowest JS divergence values and the highest CPC value), indicating that it can generate synthetic trajectories aligning statistically closer with the real data. Specifically, *Duration*, *LocNum* and *I-rank* are mainly determined by the activity-sequence generation model, reflecting that Transformer with prior-clustering can help capture and preserve the temporal patterns of the real data. While the good performance of space-related metrics at individual level (i.e., *Radius*, *Displacement*) and collective level (i.e., *CPC*) reflects the effectiveness of our proposed spatial-location selection model in reproducing the spatial distribution of the real data.

From those results, we can see that the combination of machine learning and mechanistic models can achieve better performance than using solely machine learning or mechanistic models. Both types of models in Act2Loc have leveraged their strengths at the right places. Moreover, Act2Loc can generate trajectories using only a smaller size of individual activity-sequence data and population distribution data, which has a low requirement for data.

Table 5. Performance comparison of Act2Loc and baseline models.

Model type	Model	JS Divergence					CPC
		<i>Duration</i>	<i>LocNum</i>	<i>I-rank</i>	<i>Radius</i>	<i>Displacement</i>	
Mechanistic models	DITRAS	0.0113	0.3629	<u>0.0020</u>	<u>0.0112</u>	0.0165	0.2926
	w-EPR	0.4771	0.6920	0.0108	0.4476	0.0120	0.0910
Machine learning models	LSTM	<u>0.0087</u>	0.4143	0.0920	0.2851	<u>0.0026</u>	0.3798
	SeqGAN	0.0125	<u>0.0330</u>	0.0162	0.1960	0.0895	<u>0.4534</u>
	MoveSim	0.1623	0.6930	0.0039	0.6710	0.1898	0.0079
Hybrid model	Act2Loc	0.0059	0.0001	0.0018	0.0016	0.0012	0.4593

5.3.3. Ablation experiments

To test the effectiveness of our proposed spatial-location selection model, we substituted the UO model with other mechanistic models for selecting “Work” and “Other” locations. Four classical models are utilized for substitution and comparison, i.e., the Gravity model (Zipf et al., 1946), the Rank-based model (Noulas et al., 2012), the Radiation model (Simini et al., 2012), and the Opportunity Priority Selection (OPS) model (Liu et al., 2019). It is worth to mention that the Radiation model (Simini et al., 2012) and the Opportunity Priority Selection (OPS) model (Liu et al., 2019) are also intervening-opportunity-based models and are covered by the UO model using its two parameters (α , β). When $\alpha = 0$ and $\beta = 1$, the UO model is equivalent to the Radiation model, while when $\alpha = 1$ and $\beta = 0$, the UO model is equivalent to the OPS model.

Table 6 displayed the trajectory generation results based on the five different mechanistic models with individual activity sequences generated by the same model introduced in Section 4.1. We can see that metrics such as *Duration*, *LocNum* and *I-rank* seem not to be related to the choice of mechanistic models. This is because those metrics have been determined once the activity sequences have been generated. As for space-related metrics, such as *Radius*, *Displacement* and *CPC*, the UO model exhibits the best performance than other mechanistic models, indicating that it can better reproduce the spatial distributions of the real data. This may be because the UO model covers and balances the Radiation model and OPS model using its parameters (α , β) and can better predict human mobility by taking both advantages of the two models.

Table 6. Ablation of different mechanistic models in spatial-location selection model.

Model	JS Divergence					CPC
	<i>Duration</i>	<i>LocNum</i>	<i>I-rank</i>	<i>Radius</i>	<i>Displacement</i>	
Gravity model	0.0059	0.0001	0.0018	0.0372	0.0351	0.2459
Rank-based model	0.0059	0.0001	0.0018	0.0247	0.0402	0.3665
Radiation model	0.0059	0.0001	0.0018	0.0146	0.0241	0.3899
OPS model	0.0059	0.0001	0.0018	0.0326	0.0398	0.3674
UO model	0.0059	0.0001	0.0018	0.0016	0.0012	0.4593

5.3.4. Visualization analysis

Figure 6 illustrates four generated individual trajectories of a week under the four activity patterns shown in Figure 5(b). To conveniently compare those trajectories, we selected individuals living at Minzhi Street (marked as a red dot) and working (if applicable) at Futian Street (marked as a blue dot). Figures 6(a) demonstrate an individual trajectory without a workplace outside the home location. In such situation, the other activity locations are mainly concentrated around the home location, which reflects the constraint effect of the residence. Figures 6(b)-(d) demonstrate individuals who commute between their homes and workplaces but with different working hours. In these cases, other activity locations are generally distributed around the residences and workplaces, reflecting the characteristic that individuals' other activity locations, such as dining and recreation, are typically constrained by their residences and workplaces (Gonzalez et al., 2008; Yan et al., 2011; Wang et al., 2019). Moreover, individuals with longer working hours tend to have fewer other activity locations, and those other activity locations tend to be closer to their residences and workplaces. In contrast, individuals with shorter working hours tend to have more, consecutive, and distant other activity locations. This is because activities of “Home” and “Work” dominate human daily life, individuals with a busy work usually have limited time budgets to conduct “Other” activities in a distant place (Dijst et al., 2002). Overall, the generated trajectories' spatio-temporal characteristics are consistent with human mobility behavior in the real world.

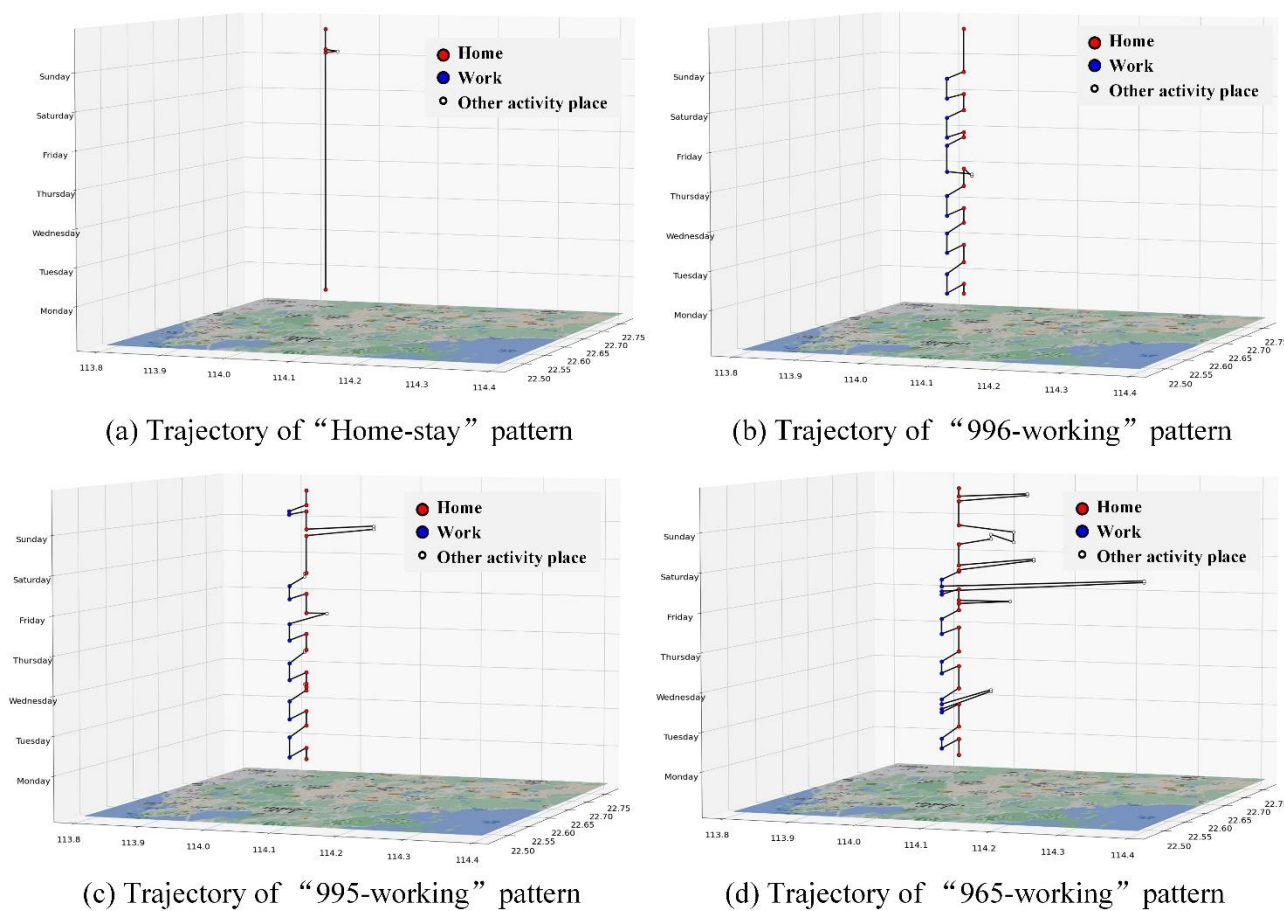


Figure 6. Illustration of generated individual trajectories under the four significant activity patterns.

6. Discussion and conclusions

This study proposes a novel trajectory generation method, Act2Loc, to generate synthetic trajectories that are statistically close with the real data. The method firstly employs machine learning models to generate individual activity sequences that can well preserve the human daily activity patterns, then applies mechanistic models to enable the spatial-explicit selection of activity locations. The combination of these models results in a high-quality and transparent spatio-temporal trajectory generation method. In addition, Act2Loc only needs small-sample individual activity sequences and population distribution data as inputs, which are easy to obtain. From a perspective of scientific theory and methodology, this approach enables us to adaptively combine and leverage the strengths of both machine learning and mechanistic models and offers new insights on the knowledge-guided GeoAI for human mobility studies. While from a perspective of practice, this method directly addresses the limitations of raw trajectory data, such as personal privacy concerns and issues related to data redundancy, missing, and noise, which can substitute the real data and be applied to applications of epidemic simulation, transportation management, digital twin city construction, etc.

In future work, we seek to improve our study from several perspectives. Firstly, we aim to enhance the modeling capability for individual mobility behavior to generate a trajectory dataset that more closely aligns with reality while maintaining low requirements for input data. Secondly, we plan to release a synthetic

trajectory generation tool that allows users to generate a specified number of trajectories based on low-cost data requirements. Thirdly, we intend to apply our method to more cities to validate and improve its transferability and robustness. Lastly, we will explore other coupling modes of machine learning and mechanistic models to better leverage their advantages in trajectory generation.

Acknowledgments

Kang Liu acknowledges supports from the National Key Research and Development Program of China (No. 2022YFB3904203) and the National Natural Science Foundation of China (No. 42271474). Shifen Cheng acknowledges support from the National Natural Science Foundation of China (No. 42371469). Ling Yin acknowledges support from the National Natural Science Foundation of China (No. 42271475). Any opinions, findings, and conclusions or recommendations expressed in this material are those of the authors and do not necessarily reflect the views of the funders. All the authors acknowledge the anonymous reviewers for providing valuable comments and suggestions.

Disclosure statement

No potential conflict of interest was reported by the authors.

Data and codes availability statement

The data and codes that used in this research are available in figshare.com with the unique identifier at the link <https://doi.org/10.6084/m9.figshare.23658450>. Two datasets are included: the individual activity-sequence data and the population distribution data. The former includes 1000 individual activity sequences in a span of a week with hourly time intervals. The latter includes the shapefile of the 1km-grids and the corresponding population distribution. The raw mobile positioning data cannot be shared publicly since they compromise individual privacy.

Funding

This work was supported by the National Key Research and Development Program of China [2022YFB3904203]; National Natural Science Foundation of China [42271474, 42371469, 42271475].

Notes on contributors

Kang Liu is an Associate Professor at the Shenzhen Institute of Advanced Technology, Chinese Academy of Sciences. She received her Ph.D. in Geographic Information Science from the Institute of Geographic Sciences and Natural Resources Research (IGSNRR), Chinese Academy of Sciences (CAS) in 2018. Her research interests mainly focus on human mobility modeling and Geospatial Artificial Intelligence (GeoAI).

Xin Jin is currently pursuing a master's degree in computer science at the Shenzhen Institute of Advanced Technology (SIAT), Chinese Academy of Sciences (CAS). His research interests focus on human mobility modeling and spatiotemporal data mining.

Shifen Cheng is an Associate Professor at the Institute of Geographic Sciences and Natural Resources Research (IGSNRR), Chinese Academy of Sciences (CAS). His research interests mainly focus on interpolation,

reconstruction, and prediction methods for heterogeneous and sparsely distributed geospatial data.

Song Gao is an Associate Professor in GIScience at the Department of Geography, University of Wisconsin-Madison. He holds a Ph.D. in Geography from the University of California Santa Barbara. His research interests include place-based GIS, geospatial data science, human mobility, and social sensing.

Ling Yin is a Professor at the Shenzhen Institute of Advanced Technology (SIAT), Chinese Academy of Sciences (CAS). She received her Ph.D. from the University of Tennessee at Knoxville in 2011. Her research interest mainly focuses on spatially epidemic modeling and spatiotemporal data mining.

Feng Lu is a Professor at the Institute of Geographic Sciences and Natural Resources Research (IGSNRR), Chinese Academy of Sciences (CAS). His research interests cover spatiotemporal data modeling, spatiotemporal knowledge graph, computational transportation science, and location-based services.

ORCID

Kang Liu <https://orcid.org/0000-0001-7466-4123>

Song Gao <http://orcid.org/0000-0003-4359-6302>

Ling Yin <https://orcid.org/0000-0002-0262-0655>

Reference

- [1] Alessandretti, L., et al. 2018. Evidence for a conserved quantity in human mobility. *Nature Human Behaviour*, 2(7), 485-491. doi:10.1038/s41562-018-0364-x.
- [2] Ari H., et al. 2018. Learning to write with cooperative discriminators. In *Proceedings of the 56th Annual Meeting of the Association for Computational Linguistics*. doi:10.18653/v1/P18-1152
- [3] Anastasiou, C., Kim, S. H. and Shahabi, C., 2022. Generation of Synthetic Urban Vehicle Trajectories. In *2022 IEEE International Conference on Big Data (Big Data)*. IEEE. doi:10.1109/bigdata55660.2022.10020237.
- [4] Baraglia, R., et al. 2013. LearNext: learning to predict tourists movements. In *Proceedings of the 22nd ACM international conference on Information & Knowledge Management*. ACM. doi:10.1145/2505515.2505656.
- [5] Bandara, K., Bergmeir, C., and Smyl, S. 2020. Forecasting across time series databases using recurrent neural networks on groups of similar series: A clustering approach. *Expert systems with Applications*, 140, 112896.
- [6] Barbosa, H., et al. 2015. The effect of recency to human mobility. *EPJ Data Science*, 4, 1-14. doi:10.1140/epjds/s13688-015-0059-8.
- [7] Barbosa, H., et al. 2018. Human mobility: Models and applications. *Physics Reports*, 734, 1-74. doi:10.1016/j.physrep.2018.01.001.
- [8] Berke A, et al. 2022. Generating synthetic mobility data for a realistic population with RNNs to improve utility and privacy. In *Proceedings of the 37th ACM/SIGAPP Symposium on Applied Computing*, 964-967. doi: 10.1145/3477314.3507230.
- [9] Brockmann, D., Hufnagel, L. and Geisel, T. 2006. The scaling laws of human travel. *Nature*, 439(7075), 462-465. doi: 10.1038/nature04292.
- [10] Chen, C., et al. 2016. The promises of big data and small data for travel behavior (aka human mobility) analysis. *Transportation Research Part C: Emerging Technologies*, 68, 285-299. doi: 10.1016/j.trc.2016.04.005.

- [11] Chen, M., Liu, Y. and Yu, X., 2014. NLPMM: A next location predictor with Markov modeling. In *Advances in Knowledge Discovery and Data Mining: 18th Pacific-Asia Conference, PAKDD 2014*. Springer International Publishing, 186-197. doi:10.1007/978-3-319-06605-9_16.
- [12] Choi, S et al. 2021. TrajGAIL: Generating urban vehicle trajectories using generative adversarial imitation learning. *Transportation Research Part C: Emerging Technologies*, 128, 103091. doi: 10.1016/j.trc.2021.103091.
- [13] Cornacchia, G. and Pappalardo, L. 2021. STS-EPR: Modelling individual mobility considering the spatial, temporal, and social dimensions together. *Procedia Computer Science*, 184, 258-265. doi:10.1016/j.procs.2021.03.035.
- [14] Dijst, M. and Vidakovic, V. 2000. Travel time ratio: the key factor of spatial reach. *Transportation*, 27(2), 179-199. doi:10.1023/a:1005293330869.
- [15] Dodge, S., et al. 2020. Progress in computational movement analysis – towards movement data science. *International Journal of Geographical Information Science*, 34(12), 2395-2400. doi:10.1080/13658816.2020.1784425.
- [16] Eagle, N. and Pentland, A. S. 2009. Eigenbehaviors: identifying structure in routine. *Behavioral Ecology and Sociobiology*, 63(7), 1057-1066. doi:10.1007/s00265-009-0739-0.
- [17] Feng, J., et al., 2018. DeepMove: Predicting human mobility with attentional recurrent networks. In *Proceedings of the 2018 World Wide Web Conference on World Wide Web*. ACM Press. doi:10.1145/3178876.3186058.
- [18] Feng, J., et al., 2020. Learning to simulate human mobility. In *Proceedings of the 26th ACM SIGKDD International Conference on Knowledge Discovery & Data Mining*. ACM. doi:10.1145/3394486.3412862.
- [19] Gambs, S., Killijian, M.-O. and Del Prado Cortez, M. N., 2012. Next place prediction using mobility Markov chains. In *Proceedings of the First Workshop on Measurement, Privacy, and Mobility*. ACM. doi:10.1145/2181196.2181199.
- [20] González, M. C., Hidalgo, C. A. and Barabási, A. L. 2008. Understanding individual human mobility patterns. *Nature*, 453(7196), 779-782. doi:10.1038/nature06958.
- [21] Huang D, et al. 2019. A variational autoencoder based generative model of urban human mobility. In *2019 IEEE Conference on Multimedia Information Processing and Retrieval (MIPR)*. IEEE Computer Society. doi: 10.1109/MIPR.2019.00086.
- [22] Ikanovic, E. L. and Mollgaard, A. 2017. An alternative approach to the limits of predictability in human mobility. *EPJ Data Science*, 6(1). doi:10.1140/epjds/s13688-017-0107-7.
- [23] Ji, Y., et al. 2023. Rethinking the regularity in mobility patterns of personal vehicle drivers: A multi-city comparison using a feature engineering approach. *Transactions in GIS*, 27(3), 663-685. doi:10.1111/tgis.13043.
- [24] Jiang, S., et al. 2016. The TimeGeo modeling framework for urban motility without travel surveys. *Proceedings of the National Academy of Sciences*, 113(37), E5370-E5378. doi:10.1073/pnas.1524261113.
- [25] Jiang, S., Ferreira, J. and González, M. C. 2012. Clustering daily patterns of human activities in the city. *Data Mining and Knowledge Discovery*, 25(3), 478-510. doi:10.1007/s10618-012-0264-z.
- [26] Jiang, W., et al. 2023. Continuous trajectory generation based on two-stage GAN. In *Proceedings of the AAAI Conference on Artificial Intelligence*, 37(4), 4374-4382. doi:10.1609/aaai.v37i4.25557.
- [27] Kamel Boulos, M. N., et al. 2022. Reconciling public health common good and individual privacy: new methods and issues in geoprivacy. *International Journal of Health Geographics*, 21(1), 1. doi:10.1186/s12942-022-00300-9.
- [28] Kaufman, L. and Rousseeuw, P. J. 1990. *Partitioning Around Medoids (Program PAM)*, Wiley Series in Probability and Statistics, Hoboken, NJ, USA: John Wiley & Sons, Inc., pp. 68–125. doi:10.1002/9780470316801.ch2.
- [29] Kulkarni, V., et al. 2018. Generative models for simulating mobility trajectories. arXiv preprint arXiv:1811.12801. doi: 10.48550/arXiv.1811.12801.

- [30] Levenshtein, V. I. February 1966. Binary codes capable of correcting deletions, insertions, and reversals. *Soviet Physics Doklady*. 10 (8): 707–710.
- [31] Li, M., et al. 2018. Predicting future locations of moving objects with deep fuzzy-LSTM networks. *Transportmetrica A: Transport Science*, 16(1), 119-136. doi:10.1080/23249935.2018.1552334.
- [32] Liang, X., et al. 2012. The scaling of human mobility by taxis is exponential. *Physica A: Statistical Mechanics and its Applications*, 391(5), 2135-2144. doi:10.1016/j.physa.2011.11.035.
- [33] Liu, E. and Yan, X. 2020. A universal opportunity model for human mobility. *Scientific reports*, 10(1), 4657-4657. doi:10.1038/s41598-020-61613-y.
- [34] Long, J. A., et al. 2018. Moving ahead with computational movement analysis. *International Journal of Geographical Information Science*, 32(7), 1275-1281. doi:10.1080/13658816.2018.1442974.
- [35] Luca, M., et al. 2021. A survey on deep learning for human mobility. *ACM Computing Surveys (CSUR)*, 55(1), 1-44. doi:10.1145/3485125.
- [36] Mathew, W., Raposo, R. and Martins, B., 2012. Predicting future locations with hidden Markov models. In *Proceedings of the 2012 ACM Conference on Ubiquitous Computing*. ACM. doi:10.1145/2370216.2370421.
- [37] Muntean, C. I., et al. 2015. On learning prediction models for tourists paths. *ACM Transactions on Intelligent Systems and Technology (TIST)*, 7(1), 1-34. doi:10.1145/2766459.
- [38] Noulas, A., et al. (2012). A tale of many cities: universal patterns in human urban mobility. *PloS one*, 7(5), e37027.
- [39] Ouyang, K., et al., 2018. A Non-Parametric Generative Model for Human Trajectories. In *Proceedings of the 27th International Joint Conference on Artificial Intelligence*. doi:10.24963/ijcai.2018/530.
- [40] Pappalardo, L. and Simini, F. 2018. Data-driven generation of spatio-temporal routines in human mobility. *Data mining and knowledge discovery*, 32(3), 787-829. doi:10.1007/s10618-017-0548-4.
- [41] Pappalardo, L., et al. 2023. Future directions in human mobility science. *Nature Computational Science*, 1-13. doi: 10.1038/s43588-023-00469-4.
- [42] Pappalardo, L., et al. 2015. Returners and explorers dichotomy in human mobility. *Nature communications*, 6, 8166. doi: 10.1038/ncomms9166.
- [43] Prechelt, L. 1998. Automatic early stopping using cross validation: quantifying the criteria. *Neural networks*, 11(4), 761-767. doi:10.1016/S0893-6080(98)00010-0
- [44] Qiao, S., et al. 2015. A self-adaptive parameter selection trajectory prediction approach via hidden Markov models. *IEEE Transactions on Intelligent Transportation Systems*, 16(1), 284-296. doi:10.1109/tits.2014.2331758.
- [45] Rao, J., et al., 2020. LSTM-TrajGAN: a deep learning approach to trajectory privacy protection. In *Proceedings of the 11th International Conference on Geographic Information Science (GIScience 2021) - Part I*. doi: 10.4230/LIPIcs.GIScience.2021.I.12.
- [46] Rhee, I., et al. 2011. On the levy-walk nature of human mobility. *IEEE/ACM Transactions on Networking*, 19(3), 630-643. doi:10.1109/tnet.2011.2120618.
- [47] Roth, C., et al. 2011. Structure of urban movements: polycentric activity and entangled hierarchical flows. *PloS one*, 6(1), e15923. doi:10.1371/journal.pone.0015923.
- [48] Rousseeuw, P. J. 1987. Silhouettes: a graphical aid to the interpretation and validation of cluster analysis. *Journal of Computational and Applied Mathematics*, 20, 53-65. doi: 10.1016/0377-0427(87)90125-7.
- [49] Savage, N. 2023. Synthetic data could be better than real data. *Nature*. doi:10.1038/d41586-023-01445-8.
- [50] Schläpfer, M., et al. 2021. The universal visitation law of human mobility. *Nature*, 593(7860), 522-527. doi:10.1038/s41586-021-03480-9.
- [51] Simini, F., et al. 2012. A universal model for mobility and migration patterns. *Nature*, 484(7392), 96-100. doi:10.1038/nature10856.
- [52] Song, C., et al. 2010. Modelling the scaling properties of human mobility. *Nature Physics*, 6(10), 818-823. doi:10.1038/nphys1760.

- [53] Song, X., et al. 2016. Deeptransport: prediction and simulation of human mobility and transportation mode at a citywide level. In Proceedings of the Twenty-Fifth International Joint Conference on Artificial Intelligence. AAAI Press, 2618–2624. doi: 10.5555/3060832.3060987.
- [54] Teixeira, D. D. C., et al. 2021. The impact of stationarity, regularity, and context on the predictability of individual human mobility. *ACM Transactions on Spatial Algorithms and Systems*, 7(4), 1-24. doi:10.1145/3459625.
- [55] Toole, J. L., et al. 2015. Coupling human mobility and social ties. *Journal of the Royal Society Interface*, 12(105), 20141128. doi:10.1098/rsif.2014.1128.
- [56] Vaswani, A., et al. 2017. Attention is all you need. *Advances in Neural Information Processing Systems*. Curran Associates, Inc. 30.
- [57] Wang, J., et al. 2019. An extended exploration and preferential return model for human mobility simulation at individual and collective levels. *Physica A: Statistical Mechanics and its Applications*, 534, 121921. doi:10.1016/j.physa.2019.121921.
- [58] Xia, T., et al. 2021. AttnMove: History enhanced trajectory recovery via attentional network. In Proceedings of the AAAI Conference on Artificial Intelligence, 35(5), 4494-4502. doi:10.1609/aaai.v35i5.16577.
- [59] Yan, X. Y., et al. 2011. Exact solution of the gyration radius of an individual's trajectory for a simplified human regular mobility model. *Chinese Physics Letters*, 28(12), 120506. doi:10.1088/0256-307x/28/12/120506.
- [60] Yin, L., et al. 2021. A data driven agent-based model that recommends non-pharmaceutical interventions to suppress Coronavirus disease 2019 resurgence in megacities. *Journal of the Royal Society Interface*, 18(181), 20210112. doi:10.1098/rsif.2021.0112.
- [61] Yu, L., et al., 2017. SeqGAN: sequence generative adversarial nets with policy gradient. In Proceedings of the Thirty-First AAAI Conference on Artificial Intelligence (AAAI-17). AAAI. doi: 10.5555/3298483.3298649.
- [62] Yuan, Y, et al. Activity trajectory generation via modeling spatiotemporal dynamics. In Proceedings of the 28th ACM SIGKDD Conference on Knowledge Discovery and Data Mining. 2022: 4752–4762. doi: 10.1145/3534678.3542671.
- [63] Yuan Y, et al. Spatio-temporal Diffusion Point Processes. In Proceedings of the 29th ACM SIGKDD Conference on Knowledge Discovery and Data Mining. 2023: 3173–3184. doi: 10.1145/3580305.3599511.
- [64] Yue, Y., et al. 2014. Zooming into individuals to understand the collective: A review of trajectory-based travel behaviour studies. *Travel Behaviour and Society*, 1(2), 69-78. doi:10.1016/j.tbs.2013.12.002.
- [65] Zhu, H. and Wang, F. 2021. An agent-based model for simulating urban crime with improved daily routines. *Computers, Environment and Urban Systems*, 89, 101680. doi:10.1016/j.compenvurbsys.2021.101680.
- [66] Zhu, Y., et al. Diffusion Model for GPS Trajectory Generation. arXiv preprint arXiv:2304.11582. 2023. doi:10.48550/arXiv.2304.11582.